

Pion Condensation at Finite Temperature and Density; the Role of Charge Neutrality

Jens O. Andersen* and Lars Kyllingstad†

Department of Physics, Norwegian Institute of Science and Technology, N-7491 Trondheim, Norway

(Dated: May 26, 2019)

We study the phase structure of the two-flavor Nambu-Jona-Lasinio model in the presence of baryon and isospin chemical potential at zero and finite temperature. Any finite value of the chemical potentials restores chiral symmetry, while there is a charged pion condensate for small chemical potentials which depend on temperature. We also examine the effects of imposing charge neutrality and weak equilibrium on the phase structure of the model. In this case, there is window of baryon chemical potential and temperature where the charged pions condense.

PACS numbers: 14.40.-n;11.30.Qc;12.39.-x;21.65.+f

I. INTRODUCTION

It is believed that one can calculate the properties of strongly interacting matter by using perturbative QCD at asymptotically high temperature or at asymptotically high densities. Away from these asymptotic regimes, perturbation theory is bound to fail due to non-perturbative effects and other methods must be used. Low-energy effective theories can be used to describe hadronic matter in the nonperturbative regime and one can gain insight into the phase diagram of QCD. These toy models typically share some of the properties of QCD and are used to describe some aspects of QCD in the nonperturbative regime. For example, the $O(4)$ -symmetric linear sigma model has been used extensively at finite temperature and density to describe two-flavor QCD [1, 2, 3, 4, 5, 6] and Refs. therein. One is then taking advantage of the isomorphism between the groups $SU(2) \times SU(2)$ and $O(4)$. Alternatively, one can use the Nambu-Jona-Lasinio (NJL) model to study the properties of QCD [7]. Originally, this was a model of interacting nucleons but after the development of QCD, the model has been reinterpreted as model using quark degrees of freedom [8]. The NJL model has a severe shortcoming, namely that the theory is not confining. However, it still might be a useful model in cases where chiral symmetry rather than confinement is essential. An example of this is the breaking of chiral symmetry and pions which are interpreted as Goldstone bosons.

The idea of a Bose-Einstein condensate of pions or kaons in the core of compact stars has a long history and the interest in such condensates is due to their far-reaching consequences for these objects. For example, the presence of a condensate results in enhanced neu-

trino cooling [9]. Moreover, in contrast to hadronic matter in heavy-ion collisions, bulk matter in compact stars must (on average) be electrically neutral and so a neutrality constraint must be imposed. Similarly, bulk matter must be color neutral and if the system is in a color superconducting phase, one sometimes has to impose this constraint explicitly. For example, it is automatically satisfied if one uses the QCD Lagrangian, but this is not so if one describes the system using NJL-type models. This is due to the fact that there are no gauge fields in this model and that the $SU(N_c)$ color symmetry is global [10].

It was shown recently that charged pions condensed if the isospin chemical potential is larger than the pion mass. This was done using chiral perturbation theory [11, 12, 13, 14] and lattice QCD [15, 16]. Later pion condensation and the phase diagram of two-flavor QCD have been investigated using ladder QCD [17], the chiral quark model [18], the linear sigma models [5, 6, 19], and NJL models in the mean-field approximation [5, 20, 21, 22, 23].

The advantage of models with quarks as microscopic degrees of freedom, such as the NJL model, is that one can investigate simultaneously the effects of finite baryon chemical potential and isospin chemical potential. In the present paper, we consider the two-flavor NJL model at finite baryon chemical potential and isospin chemical potentials. We compute the phase diagram at zero and finite temperature as a function of these variables. We restrict ourselves to sufficiently low values of the baryon chemical potential such that there are no superconducting phases [24, 25]. We also investigate the effects on the phase diagram by imposing electric charge neutrality and β -equilibrium, and so we extend the work of Ebert and Klimenko [21, 22] to finite temperature.

The article is organized as follows. In Sec. II, we discuss the Lagrangian and the gap equations of NJL model. In Sec. III, we discuss the phase diagram at zero as well as finite temperature. In Sec. IV, we investigate

*Electronic address: andersen@tf.phys.ntnu.no

†Electronic address: kyllingst@tf.phys.ntnu.no

the phase diagram at zero and finite temperature imposing charge neutrality and β -equilibrium. In Sec. V, we summarize and conclude.

II. LAGRANGIAN AND GAP EQUATIONS

In this section, we discuss the properties of the Lagrangian of the NJL model. One treats the interactions between the quarks as pointlike current-current interactions. The Lagrangian of the NJL model can be written as [8]

$$\mathcal{L} = \mathcal{L}_0 + \mathcal{L}_1 + \mathcal{L}_2, \quad (1)$$

where the various terms are

$$\mathcal{L}_0 = \bar{\psi}(i\gamma^\mu\partial_\mu - m_0)\psi, \quad (2)$$

$$\mathcal{L}_1 = G_1 [(\bar{\psi}\psi)^2 + (\bar{\psi}\boldsymbol{\tau}\psi)^2 + (\bar{\psi}i\gamma_5\psi)^2 + (\bar{\psi}i\gamma_5\boldsymbol{\tau}\psi)^2], \quad (3)$$

$$\mathcal{L}_2 = G_2 [(\bar{\psi}\psi)^2 - (\bar{\psi}\boldsymbol{\tau}\psi)^2 - (\bar{\psi}i\gamma_5\psi)^2 + (\bar{\psi}i\gamma_5\boldsymbol{\tau}\psi)^2], \quad (4)$$

where m_0 is the quark-mass matrix, which is diagonal in flavor space. Moreover, τ_i are the Pauli matrices, and G_1 and G_2 are coupling constants. The quark field is an isospin doublet

$$\psi = \begin{pmatrix} u \\ d \end{pmatrix}. \quad (5)$$

We take $m_u = m_d$. The Lagrangian (1) has a global $SU(N_c)$ symmetry as well as a $U(1)_B$ symmetry. In the chiral limit, the Lagrangian (1) has an $SU(2)_L \times SU(2)_R$ symmetry. Away from the chiral limit, this symmetry is reduced to $SU(2)_V$. \mathcal{L}_1 has an additional $U_A(1)$ axial symmetry. \mathcal{L}_2 is 't Hooft's instanton-induced interaction term and breaks explicitly the $U(1)_A$ axial symmetry of \mathcal{L}_1 [27]. In the following, we shall limit ourselves to study the standard NJL Lagrangian by choosing $G_1 = G_2 \equiv G/2$ [8] and so we can write

$$\mathcal{L} = \bar{\psi}(i\gamma^\mu\partial_\mu - m_0)\psi + G [(\bar{\psi}\psi)^2 + (\bar{\psi}i\gamma_5\boldsymbol{\tau}\psi)^2] \quad (6)$$

We can characterize the system described by the Lagrangian (6) by the expectation values of the different conserved charges associated with the continuous symmetries. For each conserved charge Q_i , we introduce a chemical potential μ_i . Note, however, that it is possible to specify the expectation values of different charges simultaneously only if they commute. In the present case, we introduce a chemical potential μ_B associated with the $U(1)_B$ baryon symmetry, as well as a chemical potential μ_I associated with the $SU(2)_I$ isospin group.

This is done by adding to the Lagrangian (6), the terms

$$\mathcal{L}_B = \mu_B B \bar{\psi}\gamma^0\psi, \quad (7)$$

$$\mathcal{L}_I = \mu_I I_3 \bar{\psi}\gamma^0\psi, \quad (8)$$

where $\bar{\psi}\gamma^0\psi$ and $\bar{\psi}\gamma^0\tau_3\psi$ are the corresponding baryon and isospin-charge density operators, and $I_3 = \tau_3/2$ and $B = \text{diag}(1/3, 1/3)$. We can then write the Lagrangian as

$$\mathcal{L} = \bar{\psi} [i\gamma^\mu\partial_\mu - m + \mu\gamma^0 + \delta\mu\gamma^0\tau_3] \psi + G [(\bar{\psi}\psi)^2 + (\bar{\psi}i\gamma^5\tau_i\psi)^2], \quad (9)$$

where we have defined

$$\mu \equiv \frac{\mu_B}{3}, \quad (10)$$

$$\delta\mu \equiv \frac{\mu_I}{2}. \quad (11)$$

In terms of the quark chemical potentials μ_u and μ_d , we have

$$\mu = \frac{1}{2}(\mu_u + \mu_d), \quad (12)$$

$$\delta\mu = \frac{1}{2}(\mu_u - \mu_d). \quad (13)$$

The inclusion of the isospin chemical potential, breaks the $SU_I(2)$ -symmetry of the Lagrangian to $U_B(1) \times U_{I_3}(1)$. From the path-integral representation of the free energy density \mathcal{F}

$$e^{-\beta V \mathcal{F}} = \int \mathcal{D}\psi^* \mathcal{D}\psi e^{-\int_0^\beta d\tau \int d^3x \mathcal{L}}, \quad (14)$$

the expression for the charge density can be written as

$$Q_i = -\frac{\partial \mathcal{F}}{\partial \mu_i}. \quad (15)$$

We next introduce the auxiliary fields σ and π_i by

$$\sigma = -2G\bar{\psi}\psi, \quad (16)$$

$$\pi_i = -2G\bar{\psi}i\gamma_5\tau_i\psi. \quad (17)$$

The Lagrangian (9) can now compactly be written as

$$\mathcal{L} = \bar{\psi} [i\gamma^\mu\partial_\mu - m_0 + \mu\gamma^0 + \delta\mu\gamma^0\tau_3 - \sigma - i\gamma^5\pi_a\tau_a] \psi - \frac{1}{4G} (\sigma^2 + \pi_a\pi_a). \quad (18)$$

The original Lagrangian (9) can be recovered by using the equations of motion for the fields σ and π_i to eliminate them from (18). The Lagrangian is now bilinear in the quark fields and so we can integrate them out exactly. We then obtain the following effective action

$$S_{\text{eff}} = -\frac{1}{2}N_c \text{Tr} \ln [i\gamma^\mu \partial_\mu - m_0 + \mu\gamma^0 + \delta\mu\gamma^0\tau_3 - \sigma - i\gamma^5\pi_a\tau_a] - \int d^3x \int_0^\beta \frac{1}{4G} (\sigma^2 + \pi_a\pi_a) ,$$

where the trace is over Dirac indices as well as space-time. In the mean-field approximation, we neglect the fluctuations of the quantum fields $\tilde{\sigma}$ and $\tilde{\pi}_1$. This approximation coincides with the leading order of the $1/N_c$ -expansion, where N_c is the number of colors.

We next introduce a nonzero expectation value for the fields σ and π_1 to allow for a chiral condensate and a charged pion condensate. The fields are then written as

$$\sigma = -2G\langle\bar{\psi}\psi\rangle + \tilde{\sigma} , \quad (19)$$

$$\pi_1 \equiv -2Gi\langle\bar{\psi}\gamma^5\tau_1\psi\rangle + \tilde{\pi}_1 , \quad (20)$$

where $\tilde{\sigma}$ and $\tilde{\pi}_1$ are quantum fluctuating fields. For notational simplicity, we introduce the quantities M and ρ

given by

$$M \equiv m_0 - 2G\langle\bar{\psi}\psi\rangle , \quad (21)$$

$$\rho \equiv -2Gi\langle\bar{\psi}\gamma^5\tau_1\psi\rangle , \quad (22)$$

where M is the constituent quark mass. Note that in the chiral limit, the chiral condensate breaks the $SU(2)_L \times SU(2)_R$ symmetry spontaneously down to $SU(2)_V$ in the usual manner. A nonvanishing pion condensate breaks parity as well as the global $SU(2)$ symmetry. Moreover, we can always use the remaining $U(1)$ -symmetry to rotate away any nonzero value of $\langle\bar{\psi}\gamma^5\tau_2\psi\rangle$.

Using standard techniques to evaluate the trace and using $\Omega = -\beta V S_{\text{eff}}$, where Ω is the thermodynamic potential and V is the volume of the system, we obtain

$$\Omega = \frac{(M - m_0)^2 + \rho^2}{4G} - 2N_c \int \frac{d^3p}{(2\pi)^3} \left\{ E_\rho^- + T \ln [1 + e^{-\beta(E_\rho^- - \mu)}] + T \ln [1 + e^{-\beta(E_\rho^- + \mu)}] \right. \\ \left. + E_\rho^+ + T \ln [1 + e^{-\beta(E_\rho^+ - \mu)}] + T \ln [1 + e^{-\beta(E_\rho^+ + \mu)}] \right\} , \quad (23)$$

where

$$E_\rho^\pm = \sqrt{(E \pm \delta\mu)^2 + \rho^2} , \quad (24)$$

$$E = \sqrt{p^2 + M^2} . \quad (25)$$

In the limit $T \rightarrow 0$, we obtain

$$\Omega = \frac{(M - m_0)^2 + \rho^2}{4G} - 2N_c \int \frac{d^3p}{(2\pi)^3} \left\{ E_\rho^- + (\mu - E_\rho^-)\theta(\mu - E_\rho^-) + E_\rho^+ + (\mu - E_\rho^+)\theta(\mu - E_\rho^+) \right\} , \quad (26)$$

which is in agreement with the result of Ref. [21]. The values of M and ρ are found by extremizing the thermodynamic potential Ω , that is by solving the following gap equations

$$\frac{\partial\Omega}{\partial M} = 0 , \quad (27)$$

$$\frac{\partial\Omega}{\partial\rho} = 0 . \quad (28)$$

Differentiating the effective potential (23) with respect to M and ρ , we obtain the gap equations

$$0 = \frac{M - m_0}{2G} - 2N_c M \int \frac{d^3p}{(2\pi)^3} \left\{ \frac{E^+}{EE_\rho^+} \left[1 - \frac{1}{e^{\beta(E_\rho^+ - \mu)} + 1} - \frac{1}{e^{\beta(E_\rho^+ + \mu)} + 1} \right] \right. \\ \left. + \frac{E^-}{EE_\rho^-} \left[1 - \frac{1}{e^{\beta(E_\rho^- - \mu)} + 1} - \frac{1}{e^{\beta(E_\rho^- + \mu)} + 1} \right] \right\} , \quad (29)$$

$$0 = \frac{\rho}{2G} - 2N_c \rho \int \frac{d^3p}{(2\pi)^3} \left\{ \frac{1}{E_\rho^+} \left[1 - \frac{1}{e^{\beta(E_\rho^+ - \mu)} + 1} - \frac{1}{e^{\beta(E_\rho^+ + \mu)} + 1} \right] \right. \\ \left. + \frac{1}{E_\rho^-} \left[1 - \frac{1}{e^{\beta(E_\rho^- - \mu)} + 1} - \frac{1}{e^{\beta(E_\rho^- + \mu)} + 1} \right] \right\} , \quad (30)$$

where

$$E^\pm = E \pm \delta\mu. \quad (31)$$

Taking the limit $T \rightarrow 0$, these equations reduce to those obtained by Ebert and Klimenko [21]:

$$\begin{aligned} 0 &= \frac{M - m_0}{2G} - 2N_c M \int \frac{d^3p}{(2\pi)^3} \left\{ \frac{\theta(E_\rho^+ - \mu)E^+}{E_\rho^+} + \frac{\theta(E_\rho^- - \mu)E^-}{E_\rho^-} \right\}, \\ 0 &= \frac{\rho}{2G} - 2N_c \rho \int \frac{d^3p}{(2\pi)^3} \left\{ \frac{\theta(E_\rho^+ - \mu)}{E_\rho^+} + \frac{\theta(E_\rho^- - \mu)}{E_\rho^-} \right\}. \end{aligned} \quad (32)$$

The integrals appearing in Eqs. (23), (29), and (30) are ultraviolet divergent and one may impose a three-dimensional cutoff Λ to regulate them. Alternatively, one can introduce a form factor which falls off for large momenta [26]. This ensures that the integrals converge in the ultraviolet. We follow Ref. [21] and choose an ultraviolet cutoff $\Lambda = 650$ MeV and a constituent quark mass of $M = 300$ MeV. The Dyson equation for the quark propagator gives the relation between these two parameters and the coupling constant G [8]:

$$M = m_0 + 4N_f N_c \int \frac{d^3p}{(2\pi)^3} \frac{M}{\sqrt{p^2 + M^2}}, \quad (33)$$

where N_f is the number of flavors. Given the values of Λ and M , we find in the chiral limit, $m_0 = 0$, $G = 5.01$ (GeV) $^{-2}$. In the remainder of the paper, we also set $N_f = 2$, and $N_c = 3$.

III. PHASE DIAGRAM

In this section, we study the phase diagram at zero and finite temperature without taking into account charge neutrality. Since we are not considering color superconductivity, we restrict ourselves to quark chemical potentials $\mu < 350$ MeV. The equilibrium values of M and ρ are obtained by solving numerically the gap equations (29) and (30). It turns out that the possible solutions to the gap equations are a) $M = \rho = 0$, b) $M \neq 0$, $\rho = 0$ and c) $\rho \neq 0$, $M = 0$.

A. Zero Temperature

The phase diagram of the two-flavor NJL model at zero temperature is shown in Fig. 1. In region C and D, the chiral and the isospin symmetries are restored. In region A and B, there is a charged pion condensate ρ , while the chiral condensate is vanishing. Hence any finite baryon quark potential μ and/or finite isospin chemical potential $\delta\mu$ restores chiral symmetry [5, 21]. There is in other words no region where M and ρ are nonzero

simultaneously. This is also in accordance with calculations in the linear sigma model at finite isospin chemical potential [5, 6]. The transition between phase B and C is first order and is indicated by a solid line.

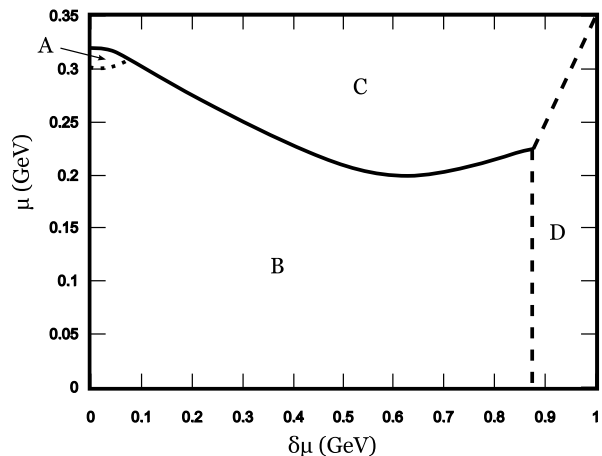


FIG. 1: Phase diagram of the two-flavor NJL model as function of quark chemical potential μ and $\delta\mu$ at zero temperature.

The difference between the regions A and B is as follows. In region B, the pion condensate depends on $\delta\mu$, but is independent of the quark potential μ . Since the baryon density is given by

$$n_B = -\frac{\partial\Omega}{\partial\mu_B}, \quad (34)$$

we conclude that the baryon density in this region vanishes. In region A, the pion condensate depends on both μ and $\delta\mu$ and so the baryon density is nonzero. The baryon density jumps discontinuously from zero to a finite value when crossing the curve. The same remark applies to region C and D, where the baryon density is nonzero only in region C. However, note that the part of the phase diagram for isospin chemical potentials $\delta\mu$ larger than the UV cutoff Λ is not necessarily reliable.

In Fig. 2, we show the pion condensate as a function of quark chemical potential for three different values of

isospin chemical potentials. It is clear that the phase transition between the broken and the symmetric phase is first order. The part of the solid line that is bending downwards corresponds to region A.

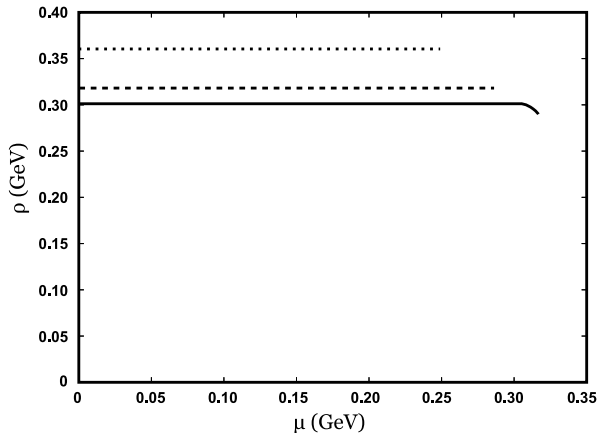


FIG. 2: Pion condensate as a function of quark chemical potential for $\delta\mu = 0$ MeV (solid line), $\delta\mu = 150$ MeV (dashed line), and $\delta\mu = 300$ MeV (dotted line) and for $T = 0$.

B. Finite Temperature

In Figs. 3–4, we show the phase diagram in the chiral limit as a function of μ and $\delta\mu$ for $T = 50$ MeV and $T = 150$ MeV. As the temperature increases, the region of pion condensation decreases. Note also that the region B shrinks as the temperature increases and eventually vanishes altogether.

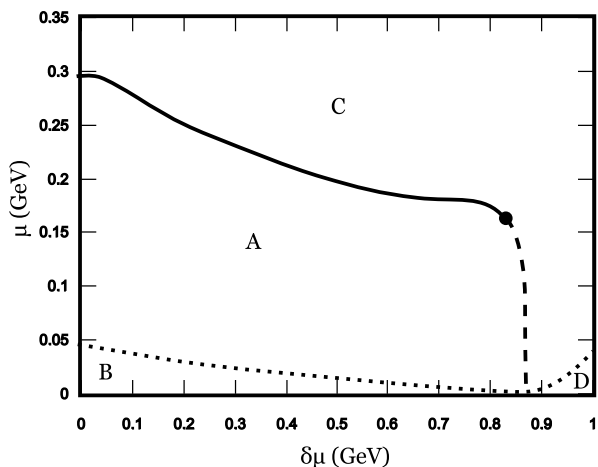


FIG. 3: Phase diagram of the two-flavor NJL model as a function of μ and $\delta\mu$ for $T = 50$ MeV.

In Figs. 5–6, we show the pion condensate as a function of quark chemical potential for three different values

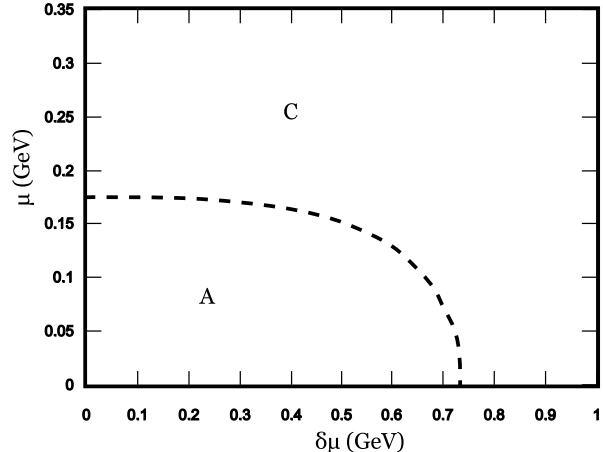


FIG. 4: Phase diagram of the two-flavor NJL model as a function of μ and $\delta\mu$ for $T = 150$ MeV.

of isospin chemical potentials and two different temperatures. It is clear that the phase transition between the broken and the symmetric phase is first order for low temperatures and second order for high temperatures (second order transitions are indicated by dashed lines). This reflects the fact that phase B disappears altogether for sufficiently high temperatures.

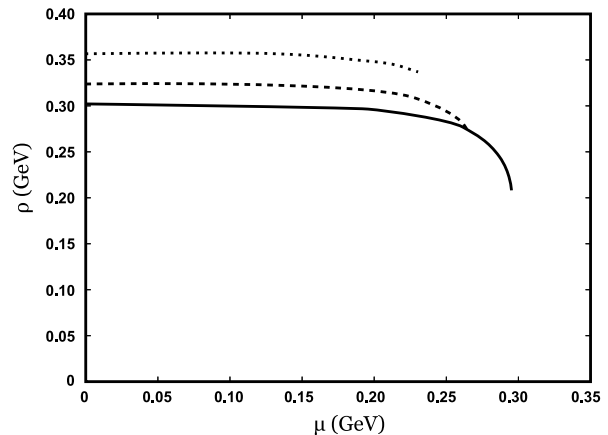


FIG. 5: Pion condensate as a function of quark chemical potential for $\delta\mu = 0$ MeV (solid line), $\delta\mu = 150$ MeV (dashed line), and $\delta\mu = 300$ MeV (dotted line) and for $T = 50$ MeV.

IV. ELECTRIC CHARGE NEUTRALITY AND β -EQUILIBRIUM

In the previous section, we have calculated the phase diagram by finding the solutions to the gap equations (27) and (28). Dense matter inside stars should be neutral with respect to electric as well as color

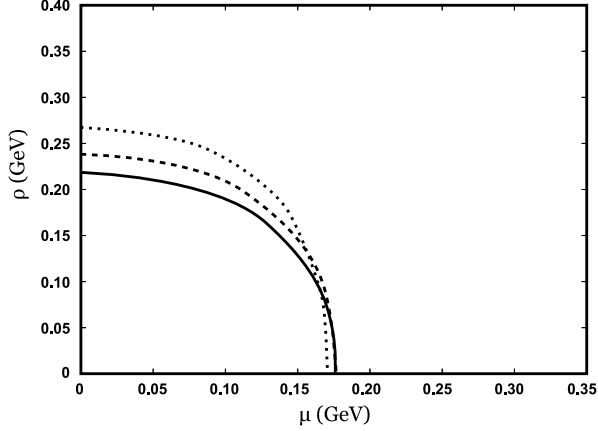


FIG. 6: Pion condensate as a function of quark chemical potential μ for $\delta\mu = 0$ MeV (solid line) $\delta\mu = 150$ MeV (dashed line), and $\delta\mu = 300$ MeV (dotted line) and for $T = 150$ MeV.

charge, otherwise one would pay an enormous energy price [25]. Since we are not considering color superconducting phases, color neutrality is automatically satisfied, while we have to impose electric charge neutrality (see e.g. Ref. [28] for a similar calculation including color superconducting phases).

In addition to charge neutrality, matter should also be in β equilibrium, that is weak-interaction processes such as

$$u \leftrightarrow d + e^+ + \nu, \quad (35)$$

should go with the same rates in both directions. If we assume that the neutrinos can leave the system, their chemical potential μ_ν vanishes. In chemical equilibrium, Eq. (35) implies

$$\mu_u = \mu_d + \mu_Q, \quad (36)$$

where μ_u and μ_d are chemical potentials for the up and down quarks, respectively. The quark chemical potentials μ_u and μ_d , and the electron chemical potential μ_e can be written in terms of the quark chemical potential μ and the electric chemical potential μ_Q :

$$\mu_u = \mu + \frac{2}{3}\mu_Q, \quad (37)$$

$$\mu_d = \mu - \frac{1}{3}\mu_Q, \quad (38)$$

$$\mu_e = -\mu_Q, \quad (39)$$

and so the system can be described in terms of the two independent chemical potentials μ and μ_Q . Once we have picked a value for μ , the solutions to the gap equations (27) and (28) and the neutrality constraint determine the chiral condensate M , charged pion condensate ρ , and the electron chemical potential μ_Q .

In order to impose the constraint of charge neutrality we require additionally that

$$\frac{\partial\Omega}{\partial\mu_Q} = 0. \quad (40)$$

The constraint (40) implies that there is only one independent chemical potential, for example μ . Note that the chemical potential appearing in Eq. (23) is half the sum of the quark chemical potentials μ_u and μ_d , and so according to Eqs. (37) and (38), we need to make the substitution $\mu \rightarrow \tilde{\mu} = \mu + \mu_Q/6$. In the remainder, we also will replace $\delta\mu$ by $\mu_Q/2$, which follows from Eqs. (13), (37), and (38).

In the following, we describe the electrons by a noninteracting fermi gas. We then add to the Lagrangian (9), the term

$$\mathcal{L}_{\text{electrons}} = \tilde{\psi}_e (\gamma^\mu \partial_\mu + \gamma^0 \mu_e e - m_e) \psi_e, \quad (41)$$

where ψ_e denotes the electron field, e is the electron charge, and m_e is the mass of the electron. The thermodynamic potential for the electrons is then

$$\Omega_{\text{electrons}} = -2 \int \frac{d^3p}{(2\pi)^3} \left\{ E_p + \ln \left[1 + e^{-\beta(E_p - \mu_Q)} \right] + \ln \left[1 + e^{-\beta(E_p + \mu_Q)} \right] \right\}, \quad (42)$$

where $E_p = \sqrt{p^2 + m_e^2}$. In the case of massless electrons, one can evaluate the integrals in Eq. (42) and one finds:

$$\Omega_{\text{electrons}} = -\frac{\mu_Q^4}{12\pi^2} - 2\frac{\mu_Q^2 T^2}{6} + \frac{7\pi^2}{720} T^4. \quad (43)$$

Adding the electron contribution Eq (43) to Eq. (23) and differentiating with respect to μ_Q , we obtain

$$0 = \frac{\mu_Q^3}{3\pi^2} + \frac{1}{6}\mu_Q T^2 + \int \frac{d^3p}{(2\pi)^3} \left\{ \frac{E^+}{E_\rho^+} - \frac{E^-}{E_\rho^-} + \left(1 - 3\frac{E^+}{E_\rho^+} \right) \frac{1}{e^{\beta(E_\rho^- - \tilde{\mu})} + 1} - \left(1 + 3\frac{E^+}{E_\rho^+} \right) \frac{1}{e^{\beta(E_\rho^- + \tilde{\mu})} + 1} + \left(1 + 3\frac{E^-}{E_\rho^-} \right) \frac{1}{e^{\beta(E_\rho^+ - \tilde{\mu})} + 1} - \left(1 - 3\frac{E^-}{E_\rho^-} \right) \frac{1}{e^{\beta(E_\rho^+ + \tilde{\mu})} + 1} \right\}. \quad (44)$$

In the zero-temperature limit, Eq. (44) reduces to that obtained by Ebert and Klimenko [22]:

$$0 = \frac{\mu_Q^3}{3\pi^2} + \int \frac{d^3p}{(2\pi)^3} \left\{ \theta(\tilde{\mu} - E_\rho^+) + \theta(\tilde{\mu} - E_\rho^-) + 3\theta(E_\rho^+ - \tilde{\mu}) \frac{E^+}{E_\rho^+} + \theta(E_\rho^- - \tilde{\mu}) \frac{E^-}{E_\rho^-} \right\}. \quad (45)$$

V. PHASE DIAGRAM REVISITED

In this section, we calculate the phase diagram of the two-flavor NJL model as a function of μ and μ_Q imposing the electric charge neutrality constraint (40). Again the solutions to the gap equations are a) $M = \rho = 0$, b) $M \neq 0$, $\rho = 0$ and c) $\rho \neq 0$, $M = 0$.

A. Zero Temperature

In Fig 7. we show the electric chemical potential μ_Q as a function of the quark chemical potential μ . We see that for chemical potential smaller than a critical value $\mu_{1c} = 301\text{MeV}$, the electric chemical potential vanishes. The charged pion condensate vanishes and the system is already neutral, so it is not necessary to neutralize it. In this phase, the chiral condensate is nonzero and so chiral symmetry is broken. For chemical potentials satisfying $\mu_{1c} < \mu < \mu_{2c}$, where $\mu_{2c} = 323 \text{ MeV}$, the pion condensate is nonvanishing, while the chiral condensate is zero. In this phase, the baryon density is nonzero as well. The electric charge of the baryons are neutralized by both the presence of the pion condensate and the electrons. Finally, for chemical potentials larger than μ_{2c} , the system is in the normal phase, where both condensate vanish. The baryon density is nonzero and its electric charge is neutralized by the presence of the electrons alone. As pointed out in Ref. [22], the thermodynamic potential depends on the single variable $\sqrt{M^2 + \rho^2}$ if $\mu_Q = 0$ and not on M and ρ separately. The potential then has a mexican-hat shape in the (M, ρ) -space. One therefore has the freedom to choose the values of M and ρ . Since parity is conserved in QCD at $\mu_Q = 0$, we choose $\rho = 0$ to ensure this [22]. In Fig. 8, we show the chiral condensate and the pion condensate as a function of quark chemical potential at $T = 0$. Again ρ jumps discontinuously and the phase transition is first order.

B. Finite Temperature

In Fig. 9, we show the phase diagram of neutral matter as a function of temperature T and quark chemical potential. In phase A, the pion condensate vanishes, while the chiral condensate takes the value $M \approx 300 \text{ MeV}$. In this phase, the baryon and isospin densities are zero and there is thus no electric charge in the sys-

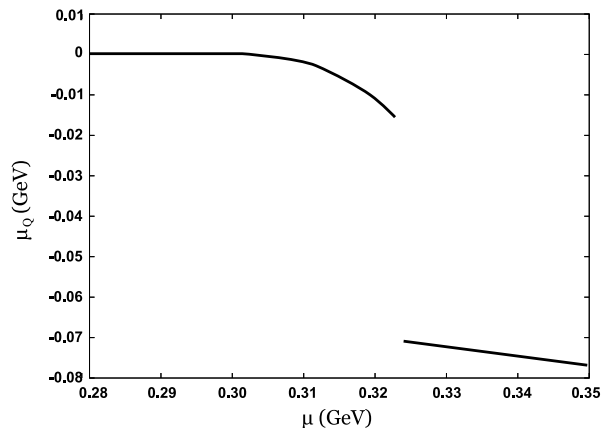


FIG. 7: Electric chemical potential μ_Q as a function of quark chemical μ in neutral matter at zero temperature.

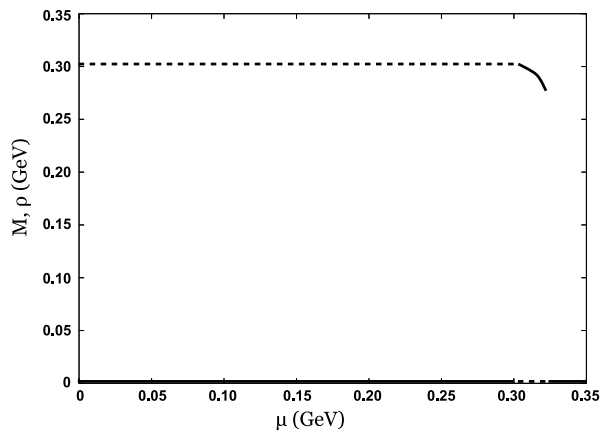


FIG. 8: Pion (solid curve) and chiral (dashed curve) condensates for neutral matter as a function of quark chemical potential μ at zero temperature.

tem. The electric chemical potential μ_Q and therefore the electron density vanishes. In phase B, the pion condensate and baryon density are nonzero, while the chiral condensate is vanishing. Once there is a nonzero pion condensate, chiral symmetry is restored and this is in accordance with calculations performed using the linear $O(4)$ model [5, 6]. In this phase, the electric chemical potential and hence the electron density is nonvanishing. The electron density and the charged pion condensate neutralize the electric charge of the charge. In phase C, we are in the normal baryonic phase with a nonzero baryon density and vanishing condensates. The

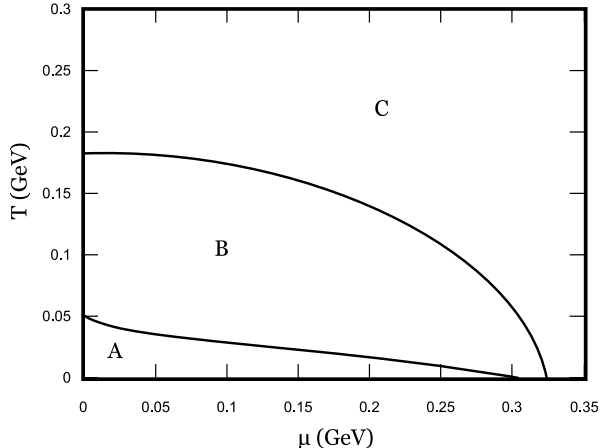


FIG. 9: Phase diagram for neutral matter as a function of T and quark chemical potential μ .

electric chemical potential is nonzero and the electrons neutralize the electric charge of the quarks. Finally, we note that the two critical chemical potentials μ_{1c} and μ_{2c} vanish at a temperature T of 51 MeV and 183 MeV, respectively.

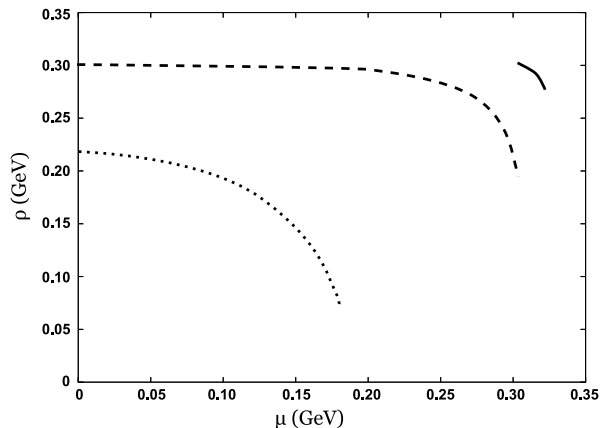


FIG. 10: Pion condensate for neutral matter as a function of quark chemical potential μ for zero temperature (solid line), $T = 50\text{MeV}$ (dashed curve) and $T = 150\text{MeV}$ (dotted curve).

In Fig. 10, we show the pion condensate for neutral matter as a function of μ for $T = 0$, $T = 50$ MeV, and $T = 150$ MeV.

VI. SUMMARY AND OUTLOOK

In this paper, we have calculated the phase diagram of the two-flavor NJL model as function of quark and isospin chemical potential, and temperature in the chiral limit. We have also imposed the constraints of electric charge neutrality and weak equilibrium.

A straightforward extension of this work is to include a nonzero constituent quark mass m_0 . Such a calculation would be similar to what was done in Ref. [20]. In Ref. [22], the authors calculate the phase diagram of neutral matter with another set of parameters at zero temperature. Using an ultraviolet cutoff of 600MeV, a coupling constant $G = 6.82(\text{GeV})^{-2}$, and a constituent quark mass of 400MeV, their numerical analysis shows that phase structure differs qualitatively from the first set of parameters. In this case there is no phase with a pion condensate, but a phase transition directly from a phase of broken chiral symmetry to a chirally symmetric phase at a critical baryon chemical potential of $\mu_c = 386.2\text{MeV}$. This seems to indicate that some features of the phase diagram are not robust and more work needs to be done to obtain qualitatively reliable results. One possibility is to include $1/N$ corrections, where N is either the number of colors or flavors [29].

Acknowledgment

J.O.A. would like to thank D. Boer and H. J. Warringa for useful discussions and suggestions.

-
- [1] S. Chiku and T. Hatsuda Phys. Rev. D **58**, 076001 (1998).
 - [2] N. Petropoulos, J. Phys. **G25**, 2225 (1999).
 - [3] J. T. Lenaghan and D. H. Rischke, J. Phys. **G26**, 431 (2000).
 - [4] J. O. Andersen, D. Boer, and H. J. Warringa, Phys. Rev. D **70**, 116007 (2004).
 - [5] L. He, M. Jin, and P. Zhuang, Phys. Rev. D **71**, 116001 (2005).
 - [6] J. O. Andersen, hep-ph/0609020.
 - [7] Y. Nambu and G. Jona-Lasinio. Phys. Rev. **122**, (345) (1961).
 - [8] M. Buballa, Phys. Rept. **407**, 205 (2005).
 - [9] D. Page and S. Reddy, astro-ph/0608360.
 - [10] D. D. Dietrich and D. H. Rischke, Prog. Part. Nucl. Phys. **53**, 305 (2004); M. Buballa and I. A. Shovkovy, Phys. Rev. D **72**, 097501 (2005).
 - [11] D. T. Son and M. Stephanov, Phys. Rev. Lett. **86**, 592 (2001).
 - [12] K. Splittorff, D. T. Son and M. Stephanov, Phys. Rev.

- D **64** 016003 (2001).
- [13] J. B. Kogut and D. Toublan, Phys. Rev. D **64** 034007 (2001).
- [14] M. Loewe and C. Villavicencio, Phys. Rev. D **67**, 074034 (2003); ibid D **70**, 074005 (2004); ibid D **71**, 094001 (2005).
- [15] J. B. Kogut and D. K. Sinclair, Phys. Rev. D **64** 014508 (2002); ibid D **66** 34505 (2002).
- [16] S. Gupta, hep-lat/0202005.
- [17] A. Barducci, R. Casalbuoni, G. Pettini, and L. Ravagli, Phys. Lett. **B564**, 217 (2003).
- [18] A. Jakovac, A. Patkos, Zs. Szep, and P. Szepfalusy, Phys. Lett. **B582**, 179 (2004).
- [19] H. Mao, N. Petropoulos, and W.-Q. Zhao, J. Phys. **G32**, 2187 (2006).
- [20] A. Barducci, R. Casalbuoni, G. Pettini, and L. Ravagli, Phys. Rev. D **69**, 096004 (2004).
- [21] D. Ebert and K.G. Klimenko, J. Phys. G Nucl. Part. Phys. **32** 599 (2006).
- [22] D. Ebert and K.G. Klimenko, J. Phys. G Nucl. Part. Eur. Phys. J. C **46**, 771 (2006).
- [23] S. Lawley, W. Bentz, and A. W. Thomas, Phys. Lett. **B632**, 495 (2006).
- [24] M. Huang and I. A. Shovkovy, Nucl. Phys. **A729**, 835 (2003); M. Huang, Int. J. Mod. Phys. **E 14**, 675 (2005).
- [25] I. A. Shovkovy, Found. Phys. **35**, 1309 (2005).
- [26] M. Alford, K. Rajagopal, and F. Wilczek, Phys. Lett. **B422**, 247, (1998).
- [27] G. 't Hooft, Phys. Rept. **142**, 357 (1986).
- [28] H. J. Warringa, hep-ph/0606063.
- [29] J. Hufner, S.P. Klevansky, P. Zhuang, and H. Voss, Ann. Phys. **234**, 225 (1994); P. Zhuang, J. Hufner, and S.P. Klevansky Nucl. Phys. **A576**, 525 (1994).